 doi:10.20944/preprints202009.0319.v1

Article

The industrial organism *Corynebacterium glutamicum* requires mycothiol as antioxidant to resist against oxidative stress in bioreactor cultivations

Fabian Stefan Franz Hartmann [1], Lina Clermont [2], Quach Ngoc Tung [3§], Haike Antelmann [3] and Gerd Michael Seibold [1,2,*]

[1] Technical University of Denmark, Department of Biotechnology and Biomedicine, Section for Synthetic Biology; Kongens Lyngby, Denmark: fashart@dtu.dk (F.H.); gesei@dtu.dk (G.S)
[2] University of Cologne, Institute of Biochemistry, Cologne, Germany.
[3] Freie Universität Berlin, Institute of Biology-Microbiology, Berlin, Germany; qtung@zedat.fu-berlin.de (Q.T.); haike.antelmann@fu-berlin.de (H.A.)
[§] present affiliation: Institute of Biotechnology, Vietnam Academy of Science and Technology, Hanoi 10000, Vietnam
* Correspondence: gesei@dtu.dk (G.S)

Abstract: In aerobic environments, bacteria are exposed to reactive oxygen species (ROS). To avoid an excess of ROS, microorganisms are equipped with powerful enzymatic and non-enzymatic antioxidants. *Corynebacterium glutamicum*, a widely used industrial platform organism, uses mycothiol (MSH) as major low molecular weight (LMW) thiol and non-enzymatic antioxidant. In aerobic bioreactor cultivations *C. glutamicum* becomes exposed to oxygen concentrations surpassing the air saturation, which are supposed to constitute a challenge for the intracellular MSH redox balance. In this study, the role of MSH was investigated at different oxygen levels (pO_2) in bioreactor cultivations in *C. glutamicum*. Despite the presence of other highly efficient antioxidant systems, such as catalase, the MSH deficient Δ*mshC* mutant was impaired in growth in bioreactor experiments performed at pO_2 values of 30%. At a pO_2 level of 20% this growth defect was abolished, indicating a high susceptibility of the MSH-deficient mutant towards elevated oxygen concentrations. Bioreactor experiments with *C. glutamicum* expressing the Mrx1-roGFP2 redox biosensor revealed a strong oxidative shift in the MSH redox potential (E_{MSH}) at pO_2 values above 20%. This indicates, that the LMW thiol MSH is an essential antioxidant to maintain the robustness and industrial performance of *C. glutamicum* during aerobic fermentation processes.

Keywords: *Corynebacterium glutamicum*, Oxidative stress, Mycothiol, Mrx1-roGFP2, Redox potential

1. Introduction

The Gram-positive soil bacterium *Corynebacterium glutamicum* is widely used as industrial workhorse primarily for the production of L-glutamate and L-lysine [1] and has been genetically engineered as a broad platform for production of several important industrial products [2,3]. Currently, *C. glutamiucm* is mostly used for aerobic production processes, but its facultative anaerobic metabolism allows to design efficient two-stage processes for the production of reduced chemicals including an aerobic growth phase and an anaerobic production phase [4,5].

Reactive oxygen species (ROS) are generated as inescapable consequence of aerobic metabolism, caused by incomplete stepwise reduction of molecular oxygen during respiration [6,7]. ROS include superoxide anions ($O_2^{\cdot-}$), hydroxyl radicals ($OH^{\cdot}$), peroxy radicals ($ROO^{\cdot}$), alkoxy radicals ($RO^{\cdot}$) and hydrogen peroxide (H_2O_2) [6–10]. An excess of ROS leads to oxidative stress, which subsequently damages essential cell components, such as lipids, proteins and nucleic acids [11]. To avoid

 doi:10.20944/preprints202009.0319.v1

irreversible damages, aerobic living organisms possess a wide range of ROS-scavengers including enzymatic and non-enzymatic detoxification systems [12–15].

Non-enzymatic antioxidant defense systems are represented by low molecular weight (LMW) thiols, which are essential to maintain a reducing environment in the cytoplasm [16]. Eukaryotes and most Gram-negative bacteria produce glutathione (GSH) as their major LMW thiol [17]. Bacteria of the Gram-positive phylum *Actinobacteria*, including *Mycobacterium tuberculosis*, *Mycobacterium smegmatis* and *C. glutamicum*, however, utilize the GSH surrogate mycothiol (MSH) [18–21]. Upon the formation of ROS, the redox-active sulfhydryl group of MSH can either scavenge free radicals directly or function as a cofactor for antioxidant enzymes resulting in formation of oxidized mycothiol disulfide (MSSM) [14,15,22,23]. MSH can prevent overoxidation of protein thiols to sulfonic acids by forming mixed disulfides *via* a mechanism referred to as protein *S*-mycothiolation [24]. Irreversible overoxidation could cause a loss of cell viability and the requirement of the synthesis of new proteins in case of essential and abundant proteins [24,25]. Upon treatment with hypochlorite, 25 *S*- mycothiolated proteins have been identified in *C. glutamicum*, indicating its protective function during oxidative stress [26]. Consequently, the absence of MSH was shown to increase oxidative stress sensitivity indicated by an oxidized environment, an impaired growth behavior and a loss of cell viability [26–28].

Previous research regarding the physiological role of antioxidants in *C. glutamicum* exclusively used artificial oxidants to induce ROS generation rather than using conditions more relevant for production conditions such as bioreactor cultivations at different aeration rates [12,15,26–28]. Of note, ROS production rates are proportional to the collision frequency of oxygen and redox enzymes [7–9,29–31]. Especially during aerobic industrial fermentations, cells are exposed to oxygen concentrations often surpassing the air saturation. Hyperbaric oxygen was shown to be detrimental for growth patterns of various organisms e.g. *Escherichia coli*, *Bacillus subtilis* and *Saccharomyces cerevisiae* [32–34]. *C. glutamicum*, as aerobic industrial platform organism, is highly robust towards oscillations of low and high oxygen concentrations [35]. However, to the best of our knowledge, the contribution of the non-enzymatic antioxidant and main LMW thiol MSH in *C. glutamicum* to its robustness during aerobic fermentations has yet not been investigated.

Here, we studied the relevance of the non-enzymatic antioxidant MSH in the industrial platform bacterium *C. glutamicum* during aerobic batch fermentations. Bioreactor experiments revealed an impaired growth behavior in the MSH deficient *C. glutamicum* Δ*mshC* mutant upon exposure to oxygen concentrations surpassing air saturation. Application of *C. glutamicum* strains expressing the stably integrated Mrx1-roGFP2 redox biosensor [28] enabled to monitor the changes in the MSH redox potential (E_{MSH}) in C. *glutamicum* WT during bioreactor cultivations at different oxygen levels. Altogether, the results of our study demonstrate the physiological importance of MSH as non-enzymatic antioxidant in *C. glutamicum* to overcome oxidative stress during aerobic bioreactor cultivations.

2. Materials and Methods

2.1. Strains, media, and culture conditions

The strains used in this study were *C. glutamicum* ATCC13032 (WT) [36], the MSH-deficient *C. glutamicum* Δ*mshC* deletion mutant [26] and the Mrx1-roGFP2 redox biosensor expressing strains *C. glutamicum* WT_Mrx1-roGFP2 and *C. glutamicum* Δ*mshC*_Mrx1-roGFP2 [28]. *C. glutamicum* strains were pre-cultured in 2xTY medium at 30°C in 500 mL shake flasks. Prior inoculation of the main-culture, cells of an overnight culture were washed twice with 100 mM potassium phosphate buffer (pH 7.0). *C. glutamicum* main cultures were grown in CGXII minimal medium [1] supplemented with 10 g L^{-1} or 20 g L^{-1} glucose as carbon source for growth experiments in shake flasks and bioreactors, respectively.

Growth experiments in bioreactors were performed aerobically at 30°C as 1-liter cultures in 1.5-liter jars in a BIOSTAT® B fermentation system (B. Braun Biotech International) as described previously [37]. The pH was maintained at 7.0 by online measurement by using a standard pH

Preprints (www.preprints.org) | NOT PEER-REVIEWED | Posted: 14 September 2020 doi:10.20944/preprints202009.0319.v1

electrode (Mettler Toledo, Giessen) and addition of 4 M KOH and 4 M H_2SO_4. Partial oxygen pressure (pO_2) was measured online by use of a polarimetric oxygen electrode (Mettler Toledo), and was adjusted to pO_2 values provided in the text in a cascade by stirring at 200 to 800 rpm as well as by mixing N_2 and air for the inlet gas. For anaerobic condition (pO_2= 0%), 100% N_2 was used until a pO_2 of 0% was reached. When required, AF204 antifoam agent (Sigma, Missouri, U.S.A.) was added manually. The data were collected with the software MFCS (Sartorius BBI Systems, Melsungen). Growth in shake flasks and bioreactors was followed by measuring the optical density ($OD\ 600_{nm}$).

2.2. Fluorescence measurements of Mrx1-roGFP2 biosensor oxidation in vitro and in vivo

For testing suitable settings for fluorescence measurements of Mrx1-roGFP2 redox biosensor oxidation, *C. glutamicum* strains harboring genomic integrated Mrx1-roGFP2 [28], were pre-cultured in 2xTY medium until the stationary phase. For preparation of crude cell extracts, cells were harvested by centrifugation (4000 rpm, 10 min., 4°C), washed twice in potassium phosphate buffer (100 mM, pH 7.0) and finally resuspended in 1 mL of the respective buffer solution. Disruption of the cells was conducted using a Ribolyzer (Precellys TM Control Device, Bertin Technologies) at 6000 rpm, 4 times for 30 seconds each. Cell debris were removed by centrifugation (12.000 rpm, 20 min.; 4°C) and 180 µL of the supernatant transferred to black flat-bottomed 96-well microplates (Thermo Fisher Scientific, Germany) for further fluorescence analysis using a fluorescence spectrophotometer (SpectraMax iD3, Molecular Devices LLC, U.S.A). After the addition of 20 µL oxidants (50 mM diamide), reductants (100 mM DTT) and 100 mM potassium phosphate buffer for fully oxidized, fully reduced and non-treated control sample, respectively, cells were incubated for 15 min at 30°C as described previously [28]. Subsequently, excitation scans were conducted (360 nm-470 nm) by setting an emission wavelength of 510 nm. For *in vivo* fluorescence measurements, *C. glutamicum* strains expressing the Mrx1-roGFP2 biosensor were harvested by centrifugation (4000 rpm, 4 min) and washed in 100 mM potassium phosphate buffer (pH 7.0). Finally, an optical density of 40 was adjusted and 180 µL of the cell suspension transferred to black flat-bottomed 96-well microplates for fluorescence analysis. To determine the maximum and minimum oxidation ratios, 20 µL of different concentrated CHP and DTT solutions were added for oxidation and reduction of the biosensor probe, respectively, until the respective ratio reached its minimum and maximum value. For samples, 20 µL potassium phosphate buffer was added instead. Mrx1-roGFP2 fluorescence intensity was recorded at an emission intensity of 510 nm upon excitation at 380 nm and 470 nm. The corresponding biosensor oxidation degree (OxD) was calculated by normalizing to fully reduced as well as oxidized controls as described previously [28,38,39] with the following equation (1):

$$OxD = \frac{I380_{sample}\ x\ I470_{red} - I380_{red}\ x\ I470_{sample}}{I380_{sample}\ x\ I470_{red} - I380_{sample}\ x\ I470_{ox} + I380_{ox}\ x\ I470_{sample} - I380_{red}\ x\ I470_{sample}} \quad (1)$$

Here, $I380_{sample}$ and $I470_{sample}$ represent the measured fluorescence intensities received for an excitation at 380 nm and 470 nm, respectively. Fully reduced and oxidized controls are given by $I380_{red}$, $I470_{red}$ and $I380_{ox}$, $I470_{ox}$, respectively. Calculated OxD values, the standard midpoint redox potential of roGFP2 (E°`roGFP2= -280 mV) [40], Faraday constant (F: 96,485 C mol^{-1}) of electric charge per mole of electrons where 2 refers to the amount of electrons transferred during the redox reaction, the respective temperature in Kelvin (T: 303.15 K) and the universal gas constant (R: 8.314 J K^{-1} mol^{-1}) were used in order to determine the MSH redox potential (E_{MSH}) *via* the Nernst equation (2):

$$E_{MSH} = E_{roGFP2} = E^{\circ`}_{roGFP2} - \left(\frac{RT}{2F}\right) x \ln\left(\frac{1 - OxD}{OxD}\right) \quad (2)$$

2.2. Statistical analysis

Analysis of one-way variance (ANOVA) with Tukey´s test was used to assess differences of biosensor oxidation degrees derived from *C. glutamicum* WT and MSH-deficient mutant strains harboring the genetically encoded biosensor Mrx1-roGFP2. Differences were considered statistically significant when $p < 0.01$.

3. Results

3.1. The MSH-deficient mutant is susceptible to elevated oxygen concentrations

To compare growth of *C. glutamicum* WT and the Δ*mshC* mutant, batch cultivations in stirred bioreactors were performed at a pO_2 value of ≥ 30% (regulated in cascade *via* the stirring rate) and a constant pH of 7.0. These are common conditions used for production and physiological studies with *C. glutamicum* [41–44]. Growth of *C. glutamicum* WT proceeded with a rate of 0.37 h^{-1} and the cells reached a final OD_{600} of 29 after 24 hours of cultivation (Fig. 1a). Growth of the MSH-deficient Δ*mshC* mutant proceeded slower when compared to *C glutamicum* WT within the first hours of the bioreactor cultivation resulting in a cessation of growth after 4 h (Fig. 1b). During the course of cultivation with *C. glutamicum* WT, a stable pO_2 value of 30% was reached after an expected initial phase with a higher pO_2 (Fig. 1a). For the MSH deficient strain, however, the decreased oxygen demand resulted in pO_2 values always above the minimal pO_2 of 30% (Fig. 1b). This decreased oxygen demand of the Δ*mshC* mutant can be explained by the impaired growth during the first 4 h of cultivation. The rise of pO_2 after 4 h of cultivation coincidences with the stop of growth of the MSH-deficient mutant (Fig. 1b). Moreover, strong foam formation was observed at this phase of the bioreactor cultivation with the Δ*mshC* mutant. Taken together, the growth deficit of the Δ*mshC* mutant revealed its susceptibility towards elevated oxygen concentrations present already during the initial phase of the bioreactor cultivation, when a control strategy was chosen to keep pO_2 values ≥30%.

To avoid high pO_2 values during the initial phase of the cultivations, a different strategy for pO_2 control was tested for the Δ*mshC* mutant, due to its susceptibility for elevated pO_2 levels. By mixing air with nitrogen, pO_2 in the bioreactor was adjusted to different levels at an initially constant stirring rate of 400 rpm. The results showed that at a pO_2 of max 20%, growth of the Δ*mshC* mutant proceeded with slightly reduced growth rate of 0.31 h^{-1} (Fig. 1d) when compared to a growth rate of 0.37 h^{-1} (Fig. 1c) for the WT. Moreover, at a pO_2 of max 20%, *C. glutamicum* WT and Δ*mshC* mutant cells reached final optical densities of 48 and 41, respectively (Fig 1c, d).

To test for negative effects of elevated pO_2 on growing cultures in bioreactors, *C. glutamicum* WT and the Δ*mshC* mutant were cultivated initially at a pO_2 of max 20% for 3 hours until optical densities of 7 and 6, respectively (Fig. 1e, f). Subsequently, the pO_2 was increased in a single step to 40%. Whereas growth of *C. glutamicum* WT continued after the increase of pO_2 to a final OD of 28 in the course of cultivation (Fig. 1e), growth of the Δ*mshC* mutant immediately stopped resulting in a final OD of 9 (Fig. 1f). These experiments showed, that the MSH-deficient Δ*mshC* mutant is highly sensitive to pO_2 levels above 20%. As MSH protects the cells against oxidative stress, these results indicate that already at slightly increased pO_2 levels oxidative stress occurs during bioreactor cultivation.

3.2. Oxidation of the Mrx1-roGFP2 biosensor allows monitoring the changes in the MSH redox potential (E_{MSH}) in C. glutamicum

The observation that the MSH deficient Δ*mshC* mutant was impaired in growth with elevated oxygen concentrations prompted us to measure the changes in the MSH redox potential (E_{MSH}) in *C. glutamicum* during bioreactor experiments. Thus, we applied the recently developed genetically encoded Mrx1-roGFP2 biosensor, which is stably integrated in the genome of *C. glutamicum* [28]. Redox sensitive GFP2 (roGFP2) harbors two Cys residues which form a disulfide bond upon oxidation, resulting in ratiometric changes of two excitation maxima in the fluorescence excitation spectrum [45]. Mrx1 further was shown to selectively reduce *S*-mycothiolated proteins as part of the Mrx1/MSH/Mtr electron pathway [18,46]. Moreover, the Mrx1-roGFP2 fusion was well characterized as redox biosensor with respect to its selectivity towards MSSM *in vitro* [28]. Upon reaction with

Preprints (www.preprints.org) | NOT PEER-REVIEWED | Posted: 14 September 2020 doi:10.20944/preprints202009.0319.v1

MSSM, the MSH moiety is transferred to Mrx1 and roGFP2, followed by intramolecular disulfide formation in roGFP2 and the concomitant change of its fluorescence excitation maxima [28] (Fig. 2a). To define suitable settings for ratiometric fluorescence measurements, crude cell extracts of *C. glutamicum* WT_Mrx1-roGFP2 with integrated Mrx1-roGFP2 were prepared and treated with 10 mM DTT or

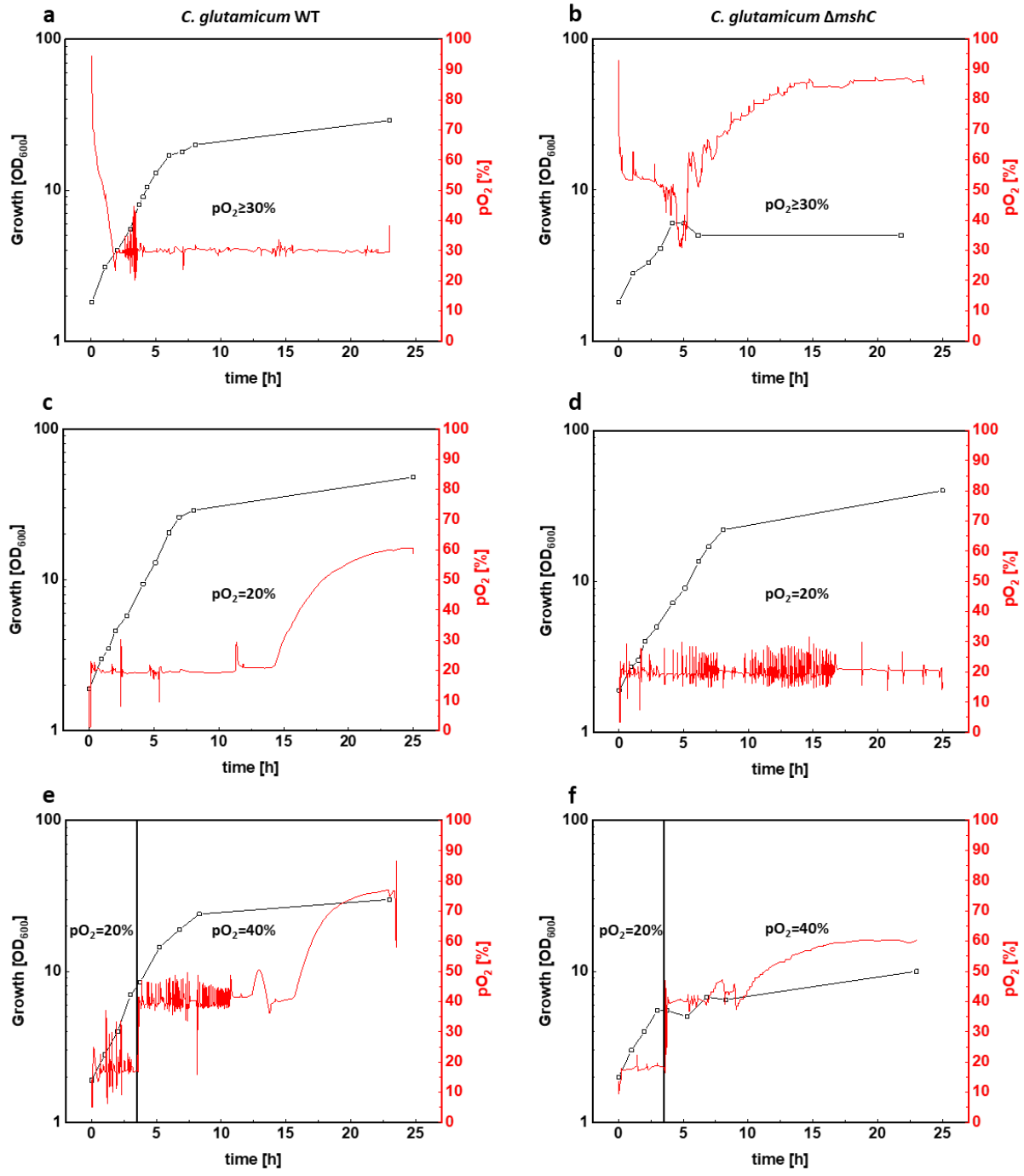

Figure 1. Batch cultivations of *C. glutamicum* WT (left plots) and the the mycothiol- deficient *C. glutamicum* mutant Δ*mshC* (right plots) in stirred bioreactors. Both strains were cultivated in 1 liter CgXII minimal medium (T= 30 °C, pH= 7.0; initial glucose concentration 20 g L-1). Bioreactor experiments were performed by setting different pO_2 values. pO_2 values of ≥30% regulated *via* stirring (200 rpm-800 rpm) **(a, b)**. pO_2 values of 20% were set by stirring as well as mixing nitrogen and air for the inlet gas **(c, d)**. Finally, bioreactor experiments were carried out with an initial pO_2 value of 20% during the first 3 hours and a second fermentation phase with a pO_2 value of 40% **(e, f)**. Growth was monitored by measuring the optical density at 600nm. Fermentations were performed in BIOSTAT® B bioreactors. Data were collected with the software MFCS.

 doi:10.20944/preprints202009.0319.v1

5 mM diamide for fully reduced and oxidized controls, respectively, as previously described [28]. The strongest fluorescence intensity alteration (emission intensity at 510 nm) under our settings was detected when the biosensor was excited at 380 nm and 470 nm (Figure A1). More specifically, upon oxidation of the probe, the excitation maximum at 380 nm increases with the subsequent decrease of the 470 nm excitation maximum and *vice versa* upon reduction of the probe. Although the second fluorescence intensity maximum was described at 488 nm previously [28], this was out of the range of measurements of our available microplate reader. Thus, we used the calculation of the 380/470 nm fluorescence intensity ratios in our biosensor settings, which is an indicator of the MSH redox potential changes in *C. glutamicum*.

For *in vivo* determination of Mrx1-roGFP2 biosensor oxidation, *C. glutamicum* WT_Mrx1-roGFP2 and Δ*mshC*_Mrx1-roGFP2, both harboring the genome integrated biosensor Mrx1-roGFP2, were cultivated in shake flasks until the stationary phase was reached. Prior fluorescence measurements, cells were harvested by centrifugation, washed twice with potassium phosphate buffer (100 mM; pH 7.0) and an optical density of 40 was adjusted as previously described [28]. Upon treatment with DTT and CHP, for reduction and oxidation of the biosensor probe, respectively, the 380/470 nm excitation ratio of Mrx1-roGFP2 was determined (Fig 2b). For non-treated samples, an equal volume of the respective buffer was added instead. Non-treated shake flask samples of *C. glutamicum* WT_Mrx1-roGFP2 and Δ*mshC*_Mrx1-roGFP2 revealed huge differences in terms of the biosensor oxidation ratio with 1.0 ±0.02 and 1.52 ±0.03, respectively (Fig. 2b). However, the addition of DTT (reducing agent) or CHP (oxidizing agent) eliminated the biosensor ratio differences resulting in fully oxidized and fully reduced biosensor ratios of 1.5-1.6 and 0.7-0.8, respectively (Fig 2b). As expected, growth of the mutant strain in shake flasks with minimal medium proceeded similar with a growth rate of 0.26 ± 0.02 h^{-1} when compared to the parental strain *C. glutamicum* WT_Mrx1-roGFP2 (0.27 ± 0.03 h^{-1}) (Fig. 2c). Biosensor measurements at the end of the exponential growth phase further revealed that the initial biosensor oxidation degrees (OxD; equation (1)) were maintained highly oxidized (0.91 ± 0.01; 0.86 ± 0.05) in the MSH-deficient mutant and more reduced (0.6 ± 0.04; 0.49 ± 0.04) in the WT strain (Fig. 2d).

This conforms a mycothiol redox potential (E_{MSH}) (equation 2) in *C. glutamicum* WT_Mrx1-roGFP2 and Δ*mshC*_Mrx1-roGFP2 of - 280 ± 2 mV and -255 ± 7 mV at the end of the exponential growth phase in shake flasks, respectively (Table 1). This observation is in accordance with the previous study, showing that *C. glutamicum* WT_Mrx1-roGFP2 maintains a highly reducing intracellular environment during the course of cultivation in shake flasks (-280 – 300 mV) [28]. In contrast, the MSH-deficient mutant showed a more oxidized intracellular environment [28]. Probably, elevated ROS levels in the MSH mutant caused an oxidation of Mrx1-roGFP2. However, in contrast to bioreactor experiments with oxygen concentrations surpassing the air saturation (pO_2= 30%), growth of the MSH-deficient mutant was not impaired in shake flasks (Fig. 2c) as seen for bioreactor cultivations with pO_2 of 20% (Fig 1d), when compared to the WT strain. This indicates, that ROS production under these conditions did not overwhelm ROS detoxification by MSH- independent enzymatic antioxidant systems in the Δ*mshC* mutant. The addition of the thiol-reactive oxidant NaOCl to shake flask cultures of the Δ*mshC* mutant was shown to be detrimental in terms of growth patterns [26], as observed during bioreactor experiments with oxygen concentrations surpassing the air saturation. This indicates the sensitivity of the Δ*mshC* mutant towards increased ROS production in bioreactors, supporting the role of MSH to overcome oxidative stress during fermentation. In contrast, MSH is not essential in aerobic shake flask cultures with lower oxygen tension, which is in agreement to the observed more reduced biosensor signals in the *C. glutamicum*_Mrx1-roGFP2 strain (Fig. 2d) [28].

Preprints (www.preprints.org) | NOT PEER-REVIEWED | Posted: 14 September 2020 doi:10.20944/preprints202009.0319.v1

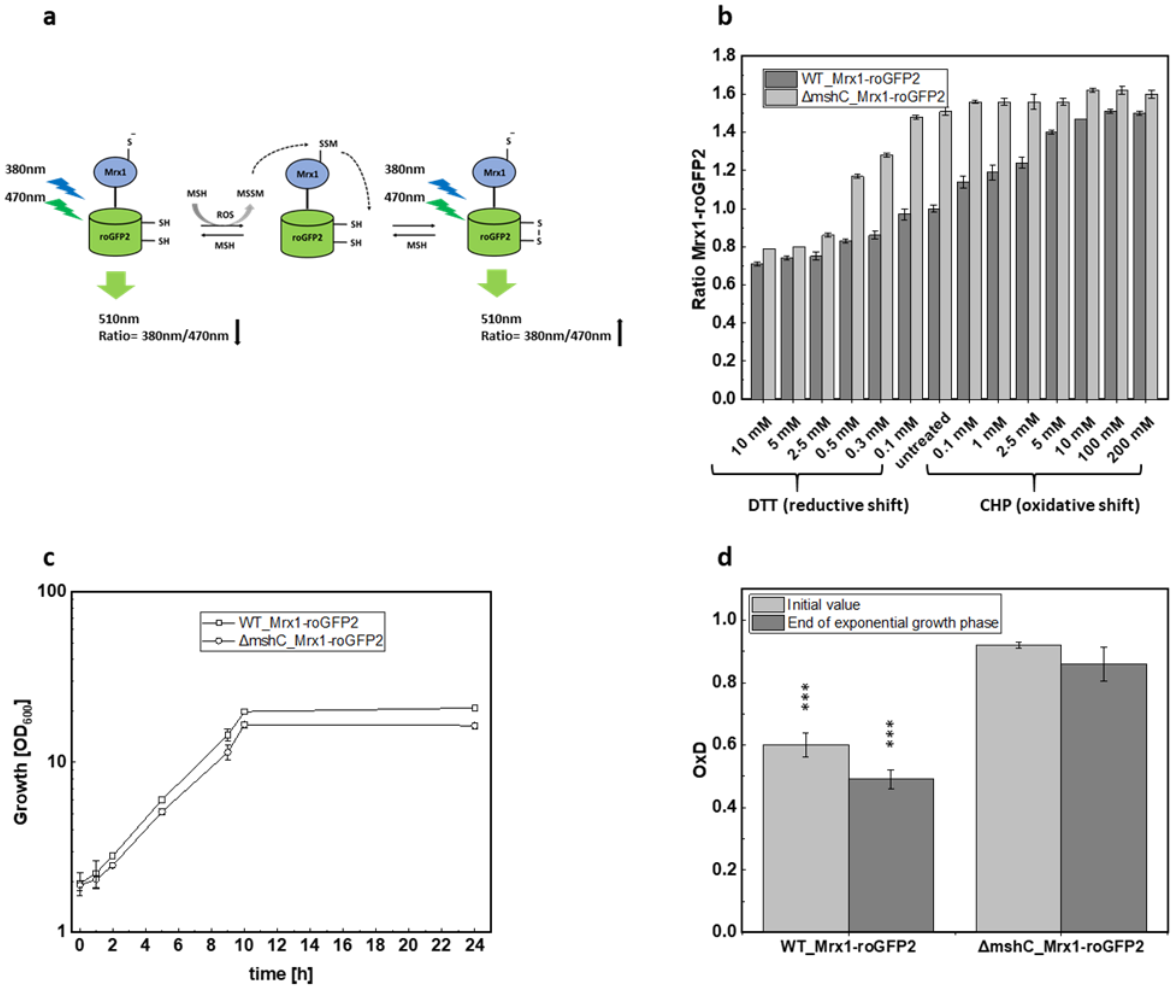

Figure 2. Schematic illustration of the Mrx1-roGFP2 biosensor response mechanism **(a)**, the ratiometric Mrx1-roGFP2 biosensor response as shown by the 380/470 nm excitation ratio upon treatment with different concentrations of reductants (DTT) and oxidants (CHP) in *C. glutamicum* WT_Mrx1-roGFP2 (WT_Mrx1-roGFP2) and *C. glutamicum* Δ*mshC*_Mrx1-roGFP2 (Δ*mshC*_Mrx1-roGFP2) **(b)**, shake flasks cultivations of WT_Mrx1-roGFP2 and Δ*mshC*_Mrx1-roGFP2 in 50 mL CGXII minimal medium (T= 30 °C, initial glucose concentration 15 g L-1 , 150 rpm) **(c)** and biosensor oxidation degrees (OxD) derived from shake flask samples after inoculation and the end of exponential growth phase **(d)**. Error bars indicate standard deviations from three independent experiments. OxD values were calculated by normalizing the samples to fully oxidized and reduced controls. OxD values of WT_Mrx1-roGFP2 are significantly different when compared to Δ*mshC*_Mrx1-roGFP2 OxD values at the p=0.01 level (one-way ANOVA with Tukey´s test) (^{ns} $p > 0.01$; * $p < 0.01$, ** $p < 0.001$, *** $p < 0.0001$).

Table 1. Mycothiol redox potential (E_{MSH}; Nernst equation) during shake flask cultivations.

Shake Flask	E_{MSH} (mV)	
	WT_Mrx1-roGFP2 [(a)]	**ΔmshC_Mrx1-roGFP2** [(b)]
Initial value	-274 ± 2	-248 ± 2
End of exponential growth phase	-280 ± 2	-255 ± 7

[(a)] *C. glutamicum* WT harboring the redox biosensor Mrx1-roGFP2. [(b)] MSH- deficient mutant of *C. glutamicum* harboring the redox biosensor Mrx1-roGFP2

 doi:10.20944/preprints202009.0319.v1

3.3 Mycothiol-dependent protection is important when C. glutamicum is exposed to elevated oxygen concentrations

To investigate the oxidative response of the Mrx1-roGFP2 biosensor in *C. glutamicum* WT_Mrx1-roGFP2 at elevated oxygen concentrations, we performed bioreactor experiments with *C. glutamicum* WT_Mrx1-roGFP2 at a pO_2 of ≥ 30%. The first fluorescence measurement revealed an almost fully oxidized biosensor.

To ensure that the biosensor response resulted from increased oxygen concentrations, the bioreactor cultivation of *C. glutamicum* WT_Mrx1-roGFP2 was performed with a stepwise pO_2 gradient (Fig. 3a). At the initial pO_2 of 0% (set by providing 100% N_2 as sole gas), the biosensor oxidation ratio was very low, indicating the presence of a reducing environment in the bioreactor at a pO_2 of 0% (Fig. 3a). Subsequently, the pO_2 value was increased in 5% steps in the bioreactor and at each of the pO_2 steps the signal ratio of the biosensor was determined 60 minutes after setting the pO_2. As depicted in Fig. 3a, the ratio of the biosensor increased when setting higher oxygen concentrations (pO_2), indicating an oxidative stress response. At a pO_2 of 30%, the biosensor oxidation degree (OxD) was determined as 0.86 ± 0.04 (Fig. 3b), representing a highly oxidized environment in *C. glutamicum* WT under these conditions. Moreover, further increase of the pO_2 value did not lead to enhanced OxD values, which are not significantly different to those determined for the MSH-deficient mutant strain (Fig. 3b). In comparison, at lower pO_2 values (pO_2=5%; pO_2=20%; pO_2=25%), OxD values determined for the WT_Mrx1-roGFP2 strain were significantly lower than the fully oxidized biosensor probes for the Δ*mshC*_Mrx1-roGFP2 mutant strain (Fig. 3b).

Notably, under aerobic conditions, the strongest oxidative shift occurred when surpassing the air saturation of 20% resulting in an OxD shift of 0.33 from 0.53 ± 0.06 (pO_2 = 20%) (which is in the range of OxD values determined for shake flask samples) towards highly oxidized values of 0.86 ± 0.04 (pO_2=30%) (Fig. 3b). This conforms an oxidative shift of E_{MSH} from -280 ± 6 mV (pO_2= 20%) to -256 ± 4 mV (pO_2 =30%) for the *C. glutamicum* WT_Mrx1-roGFP2 strain, whereas the redox potential of the mutant strain was highly oxidized at every tested pO_2 level (Table 2). This oxidative shift is in agreement with the growth defect of the MSH-deficient mutant strain when surpassing the air saturation both when setting a constant pO_2=30% (Fig. 1d), but also by a stepwise increase of the pO_2 value for the mutant strain harboring the redox biosensor Mrx1-roGFP2 (Fig. A2).

Taken together, the strong oxidative shift of *C. glutamicum* WT_Mrx1-roGFP2 in bioreactor cultivations indicates the requirement of the non-enzymatic antioxidant and LMW thiol MSH to overcome oxidative stress when the oxygen concentration surpasses the air saturation.

Preprints (www.preprints.org) | NOT PEER-REVIEWED | Posted: 14 September 2020 doi:10.20944/preprints202009.0319.v1

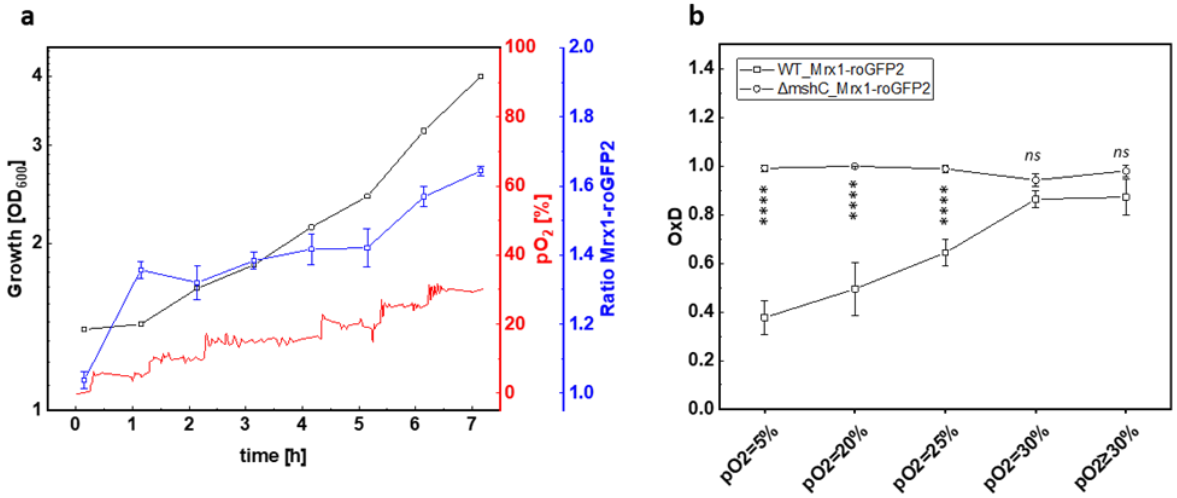

Figure 3. Growth and 380/470 nm excitation ratio of the Mrx1-roGFP2 biosensor of *C. glutamicum* WT_Mrx1-roGFP2 (WT_Mrx1-roGFP2) during batch cultivation in stirred bioreactors **(a)** and calculated oxidation degree (OxD) at different pO_2 levels during batch fermentation conducted with WT_Mrx1-roGFP2 and the MSH-deficient mutant strain *C. glutamicum* Δ*mshC*_Mrx1-roGFP2 (Δ*mshC*_Mrx1-roGFP2) **(b)**. Fermentation was performed in BIOSTAT® B bioreactors using CGXII minimal medium (T= 30 °C, pH= 7.0; initial glucose concentration 20 g L^{-1}). OxD values at respective pO_2 levels were calculated by normalizing fluorescence measurements to fully oxidized (200 mM CHP, 15 min. incubation) and reduced (10 mM DTT, 15 min. incubation) controls. Error bars indicate standard deviation of six fluorescence measurements. Significance of difference between OxD values of WT_Mrx1-roGFP2 and Δ*mshC*_Mrx1-roGFP2 at different pO_2 levels was determined by one-way ANOVA and Tukey´s test at the 0.01 level (^{ns} $p \geq 0.01$; * $p < 0.01$, ** $p < 0.001$, *** $p < 0.0001$, **** $p < 0.00001$).

Table 2. Mycothiol redox potential (E_{MSH}; Nernst equation) during bioreactor cultivations.

Bioreactor pO_2 level (%)	E_{MSH} (mV)	
	WT_Mrx1-roGFP2 [(a)]	ΔmshC_Mrx1-roGFP2 [(b)]
5	-287 ± 4	-204 ± 2
20	-280 ± 6	-191 ± 2
25	-272 ± 3	-208 ± 22
30%	-256 ± 4	-242 ± 7
≥30%	-246 ± 28	-218 ± 23

[(a)] *C. glutamicum* WT harboring the redox biosensor Mrx1-roGFP2. [(b)] MSH- deficient mutant of *C. glutamicum* harboring the redox biosensor Mrx1-roGFP2

4. Discussion

Utilization of respiratory chains for aerobic metabolism comes along with the generation of ROS [6,9]. To eliminate these toxic byproducts, aerobic organisms developed antioxidant defense mechanisms including enzymatic and non-enzymatic protection systems [12–15]. The abundant LMW thiol MSH functions to maintain the reduced state of the cytoplasm and represents the main non-enzymatic antioxidant in high-GC Gram-positive bacteria, such as the industrial platform organism *C. glutamicum* [18,26,47]. Apart from MSH, *C. glutamicum* encodes highly efficient enzymatic detoxification systems, such as the superoxide dismutase (SOD) [48], methionine sulfoxide reductases (Msr) [22,49]; catalase (KatA) and the peroxiredoxins mycothiol peroxidase (Mpx) [15,50]

 doi:10.20944/preprints202009.0319.v1

and thiol-peroxidase (Tpx) [26]. The metalloenzyme superoxide dismutase (SOD) (EC 1.15.1.1) catalyzes the dismutation of superoxide anions to dioxygen and H_2O_2. An *E. coli sodA sodB* double mutant was impaired in growth during batch cultivation when the dissolved oxygen concentration was shifted from 30% to 300% air saturation, indicating its importance in ROS detoxification during bioreactor experiments [51]. H_2O_2 subsequently is inactivated to H_2O and O_2 *via* the H_2O_2 scavenging systems KatA, Mpx and Tpx in *C. glutamicum* [15,26]. This avoids a further conversion to the highly toxic hydroxyl radical. Notably, KatA of *C. glutamicum* possesses a remarkable high activity and is even commercially available (Merck, CAS Number 9001-05-2). *C. glutamicum* was shown to be resistant towards 100 mM H_2O_2 and the Mrx1-roGFP2 biosensor did not respond to 10 mM H_2O_2 in previous studies [28]. Of note, 1-5 mM H_2O_2 resulted in a maximal roGFP2 biosensor oxidation in *E. coli* [12]. Despite the extraordinary enzymatic detoxification power of KatA, elevated oxygen concentrations during batch fermentations resulted in cell death of the MSH-deficient *C. glutamicum* mutant. ROS production rates are proportional to the collision frequency of oxygen and redox enzymes [9]. Consequently, the rate of ROS production inside the cell directly depends on the oxygen concentration in the extracellular environment [7,9]. This indicates that ROS production in bioreactor cultivations overwhelmed the remaining antioxidant systems and that MSH as additional antioxidant is required to provide protection against oxidative stress at elevated oxygen concentrations. Consistently, a strong oxidative response of the Mrx1-roGFP2 biosensor was observed when *C. glutamicum* WT was exposed to oxygen concentrations which were shown to be harmful for the MSH-deficient mutant strain in bioreactors. This confirms the requirement of MSH as supporting antioxidant and consequently an oxidative redox shift of the redox couple 2MSH/MSSM occurred in *C. glutamicum* WT strains under these conditions. MSH has multiple antioxidant functions by scavenging free radicals either directly or as a cofactor for antioxidant enzymes [18]. When the oxygen concentration surpasses the air saturation, MSH becomes a crucial player to overcome oxidative stress, despite the presence of other highly efficient enzymatic antioxidant systems working independently of MSH.

Supplementary Materials: The following supplementary figures are available online at www.mdpi.com/xxx/s1, Figure A1: Spectral scan of the Mrx1-roGFP2 biosensor of crude cell extracts of *C. glutamicum* WT_Mrx1-roGFP2, Figure A2: Growth and oxidation ratio of the biosensor Mrx1-roGFP2 of *C. glutamicum* ΔmshC_Mrx1-roGFP2 during batch cultivation in stirred bioreactors.

Author Contributions: Conceptualization, G.S. and F.H.; methodology, F.H., G.S. and L.C.; validation, F.H. and Q.T.; formal analysis, F.H. and Q.T.; investigation, F.H. G.S. and L.C.; resources, G.S. and H.A.; data curation, F.H., L.C. and G.S.; writing—original draft preparation, F.H. and G.S.; writing—review and editing, F.H., L.C., Q.T., G.S. and H.A.; visualization, F.H.; supervision, G.S; funding acquisition, G.S. and H.A. All authors have read and agreed to the published version of the manuscript.

Funding: This work was partially funded by the Novo Nordisk Fonden within the framework of the Fermentation- based Biomanufacturing Initiative (FBM) (FBM-grant: NNF17SA0031362) and by the Bio Based Industries Joint Undertaking under the European Union's Horizon 2020 research and innovation program under grant agreement No 790507 to G.S.. We further acknowledge funding by the ERC Consolidator grant (GA 615585) MYCOTHIOLOME to H.A.

Acknowledgments: We would like to thank the Fermentation Core at DTU Bioengineering for excellent technical support, Vu Van Loi (FU Berlin) for support with biosensor calculations, and Reinhard Krämer (University of Cologne) for continuous support.

Conflicts of Interest: The authors declare no conflict of interest.

References

1. Eggeling, L.; Bott, M. A giant market and a powerful metabolism: l-lysine provided by *Corynebacterium glutamicum*. *Appl. Microbiol. Biotechnol.* **2015**, *99*, 3387–3394, doi:10.1007/s00253-015-6508-2.
2. Heider, S.A.E.; Wendisch, V.F. Engineering microbial cell factories: Metabolic engineering of *Corynebacterium glutamicum* with a focus on non-natural products. *Biotechnol. J.* **2015**, *10*, 1170–1184, doi:10.1002/biot.201400590.
3. Becker, J.; Wittmann, C. Industrial Microorganisms: *Corynebacterium glutamicum*. *Ind. Biotechnol.* **2016**, 183–220, doi:10.1002/9783527807796.ch6.
4. Lange, J.; Münch, E.; Müller, J.; Busche, T.; Kalinowski, J.; Takors, R.; Blombach, B. Deciphering the adaptation of *Corynebacterium glutamicum* in transition from aerobiosis via microaerobiosis to anaerobiosis. *Genes (Basel).* **2018**, *9*, doi:10.3390/genes9060297.
5. Briki, A.; Kaboré, K.; Olmos, E.; Bosselaar, S.; Blanchard, F.; Fick, M.; Guedon, E.; Fournier, F.; Delaunay, S. *Corynebacterium glutamicum*, a natural overproducer of succinic acid? *Eng. Life Sci.* **2020**, *20*, 205–215, doi:10.1002/elsc.201900141.
6. Imlay, J.A. The molecular mechanisms and physiological consequences of oxidative stress: Lessons from a model bacterium. *Nat. Rev. Microbiol.* **2013**, *11*, 443–454, doi:10.1038/nrmicro3032.
7. Imlay, J.A. How obligatory is anaerobiosis? *Mol. Microbiol.* **2008**, *68*, 801–804, doi:10.1111/j.1365-2958.2008.06213.x.
8. Imlay, J.A. Pathways of oxidative damage. *Annu. Rev. Microbiol.* **2003**, *57*, 395–418, doi:10.1146/annurev.micro.57.030502.090938.
9. Korshunov, S.; Imlay, J.A. Detection and quantification of superoxide formed within the periplasm of *Escherichia coli*. *J. Bacteriol.* **2006**, *188*, 6326–6334, doi:10.1128/JB.00554-06.
10. Messner, K.R.; Imlay, J.A. The identification of primary sites of superoxide and hydrogen peroxide formation in the aerobic respiratory chain and sulfite reductase complex of *Escherichia coli*. *J. Biol. Chem.* **1999**, *274*, 10119–10128, doi:10.1074/jbc.274.15.10119.
11. Antelmann, H.; Helmann, J.D. Thiol-based redox switches and gene regulation. *Antioxidants Redox Signal.* **2011**, *14*, 1049–1063, doi:10.1089/ars.2010.3400.
12. Van Der Heijden, J.; Vogt, S.L.; Reynolds, L.A.; Peña-Díaz, J.; Tupin, A.; Aussel, L.; Finlay, B.B. Exploring the redox balance inside gram-negative bacteria with redox-sensitive GFP. *Free Radic. Biol. Med.* **2016**, *91*, 34–44, doi:10.1016/j.freeradbiomed.2015.11.029.
13. Seaver, L.C.; Imlay, J.A. Hydrogen peroxide fluxes and compartmentalization inside growing *Escherichia coli*. *J. Bacteriol.* **2001**, *183*, 7182–7189, doi:10.1128/JB.183.24.7182-7189.2001.
14. Si, M.; Xu, Y.; Wang, T.; Long, M.; Ding, W.; Chen, C.; Guan, X.; Liu, Y.; Wang, Y.; Shen, X.; et al. Functional characterization of a mycothiol peroxidase in *Corynebacterium glutamicum* that uses both mycoredoxin and thioredoxin reducing systems in the response to oxidative stress. *Biochem. J.* **2015**, *469*, 45–57, doi:10.1042/BJ20141080.
15. Pedre, B.; Van Molle, I.; Villadangos, A.F.; Wahni, K.; Vertommen, D.; Turell, L.; Erdogan, H.; Mateos, L.M.; Messens, J. The *Corynebacterium glutamicum* mycothiol peroxidase is a reactive oxygen species-scavenging enzyme that shows promiscuity in thiol redox control. *Mol. Microbiol.* **2015**, *96*, 1176–1191, doi:10.1111/mmi.12998.
16. Van Laer, K.; Hamilton, C.J.; Messens, J. Low-molecular-weight thiols in thiol-disulfide exchange. *Antioxidants Redox Signal.* **2013**, *18*, 1642–1653, doi:10.1089/ars.2012.4964.
17. Imber, M.; Pietrzyk-Brzezinska, A.J.; Antelmann, H. Redox regulation by reversible protein *S*-thiolation

in Gram-positive bacteria. *Redox Biol.* **2019**, *20*, 130–145, doi:10.1016/j.redox.2018.08.017.

18. Reyes, A.M.; Pedre, B.; De Armas, M.I.; Tossounian, M.A.; Radi, R.; Messens, J.; Trujillo, M. Chemistry and redox biology of mycothiol. *Antioxidants Redox Signal.* **2018**, *28*, 487–504, doi:10.1089/ars.2017.7074.
19. Tung, Q.N.; Linzner, N.; Loi, V. Van; Antelmann, H. Application of genetically encoded redox biosensors to measure dynamic changes in the glutathione, bacillithiol and mycothiol redox potentials in pathogenic bacteria. *Free Radic. Biol. Med.* **2018**, *128*, 84–96, doi:10.1016/j.freeradbiomed.2018.02.018.
20. Jothivasan, V.K.; Hamilton, C.J. Mycothiol: Synthesis, biosynthesis and biological functions of the major low molecular weight thiol in *actinomycetes*. *Nat. Prod. Rep.* **2008**, *25*, 1091–1117, doi:10.1039/b616489g.
21. Newton, G.L.; Jensen, P.R.; MacMillan, J.B.; Fenical, W.; Fahey, R.C. An N-acyl homolog of mycothiol is produced in marine *actinomycetes*. *Arch. Microbiol.* **2008**, *190*, 547–557, doi:10.1007/s00203-008-0405-3.
22. Tossounian, M.A.; Pedre, B.; Wahni, K.; Erdogan, H.; Vertommen, D.; Van Molle, I.; Messens, J. *Corynebacterium diphtheriae* methionine sulfoxide reductase a exploits a unique mycothiol redox relay mechanism. *J. Biol. Chem.* **2015**, *290*, 11365–11375, doi:10.1074/jbc.M114.632596.
23. Si, M.; Zhao, C.; Zhang, B.; Wei, D.; Chen, K.; Yang, X.; Xiao, H.; Shen, X. Overexpression of mycothiol disulfide reductase enhances *Corynebacterium glutamicum* robustness by modulating cellular redox homeostasis and antioxidant proteins under oxidative stress. *Sci. Rep.* **2016**, *6*, 1–14, doi:10.1038/srep29491.
24. Van Loi, V.; Rossius, M.; Antelmann, H. Redox regulation by reversible protein *S*-thiolation in bacteria. *Front. Microbiol.* **2015**, *6*, 1–22, doi:10.3389/fmicb.2015.00187.
25. Hillion, M.; Antelmann, H. Thiol-based redox switches in prokaryotes. *Biol. Chem.* **2015**, *396*, 415–444, doi:10.1515/hsz-2015-0102.
26. Chi, B.K.; Busche, T.; Van Laer, K.; Bäsell, K.; Becher, D.; Clermont, L.; Seibold, G.M.; Persicke, M.; Kalinowski, J.; Messens, J.; et al. Protein *S*-mycothiolation functions as redox-switch and thiol protection mechanism in *Corynebacterium glutamicum* under hypochlorite stress. *Antioxidants Redox Signal.* **2014**, *20*, 589–605, doi:10.1089/ars.2013.5423.
27. Liu, Y.; Yang, X.; Yin, Y.; Lin, J.; Chen, C.; Pan, J.; Si, M.; Shen, X. Mycothiol protects *Corynebacterium glutamicum* against acid stress via maintaining intracellular pH homeostasis, scavenging ROS, and *S*-mycothiolating MetE. *J. Gen. Appl. Microbiol.* **2016**, *62*, 144–153, doi:10.2323/jgam.2016.02.001.
28. Tung, Q.N.; Loi, V. Van; Busche, T.; Nerlich, A.; Mieth, M.; Milse, J.; Kalinowski, J.; Hocke, A.C.; Antelmann, H. Stable integration of the Mrx1-roGFP2 biosensor to monitor dynamic changes of the mycothiol redox potential in *Corynebacterium glutamicum*. *Redox Biol.* **2019**, *20*, 514–525, doi:10.1016/j.redox.2018.11.012.
29. Turrens, J.F. Mitochondrial formation of reactive oxygen species. *J. Physiol.* **2003**, *552*, 335–344, doi:10.1113/jphysiol.2003.049478.
30. Turrens, J.F.; Freeman, B.A.; Crapo, J.D. Hyperoxia increases H_2O_2 release by lung mitochondria and microsomes. *Arch. Biochem. Biophys.* **1982**, *217*, 411–421, doi:10.1016/0003-9861(82)90519-7.
31. Freeman, B.A.; Topolosky, M.K.; Crapo, J.D. Hyperoxia increases oxygen radical production in rat lung homogenates. *Arch. Biochem. Biophys.* **1982**, *216*, 477–484, doi:10.1016/0003-9861(82)90236-3.
32. Haugaard, N. Cellular mechanisms of oxygen toxicity. *Physiol. Rev.* **1968**, *48*, 311–373, doi:10.1152/physrev.1968.48.2.311.
33. Boehme, D.E.; Vincent, K.; Brown, O.R. Oxygen and toxicity inhibition of amino acid biosynthesis. *Nature* **1976**, *262*, 418–420, doi:10.1038/262418a0.
34. Gregory, E.M.; Fridovich, I. Oxygen toxicity and the superoxide dismutase. *J. Bacteriol.* **1973**, *114*, 1193–

1197, doi:10.1128/jb.114.3.1193-1197.1973.

35. Käß, F.; Hariskos, I.; Michel, A.; Brandt, H.J.; Spann, R.; Junne, S.; Wiechert, W.; Neubauer, P.; Oldiges, M. Assessment of robustness against dissolved oxygen/substrate oscillations for *Corynebacterium glutamicum* DM1933 in two-compartment bioreactor. *Bioprocess Biosyst. Eng.* **2014**, *37*, 1151–1162, doi:10.1007/s00449-013-1086-0.

36. Abe, S.; Takayama, K.I.; Kinoshita, S. Taxonomical studies on glutamic acid-producing bacteria. *J. Gen. Appl. Microbiol.* **1967**, *13*, 279–301, doi:10.2323/jgam.13.279.

37. Clermont, L.; Macha, A.; Müller, L.M.; Derya, S.M.; von Zaluskowski, P.; Eck, A.; Eikmanns, B.J.; Seibold, G.M. The α-glucan phosphorylase MalP of *Corynebacterium glutamicum* is subject to transcriptional regulation and competitive inhibition by ADP-glucose. *J. Bacteriol.* **2015**, *197*, 1394–1407, doi:10.1128/JB.02395-14.

38. Morgan, B.; Sobotta, M.C.; Dick, T.P. Measuring E_{GSH} and H_2O_2 with roGFP2-based redox probes. *Free Radic. Biol. Med.* **2011**, *51*, 1943–1951, doi:10.1016/j.freeradbiomed.2011.08.035.

39. Loi, V. Van; Harms, M.; Müller, M.; Huyen, N.T.T.; Hamilton, C.J.; Hochgräfe, F.; Pané-Farré, J.; Antelmann, H. Real-Time imaging of the bacillithiol redox potential in the human pathogen *Staphylococcus aureus* using a genetically encoded bacilliredoxin-fused redox biosensor. *Antioxidants Redox Signal.* **2017**, *26*, 835–848, doi:10.1089/ars.2016.6733.

40. Dooley, C.T.; Dore, T.M.; Hanson, G.T.; Jackson, W.C.; Remington, S.J.; Tsien, R.Y. Imaging dynamic redox changes in mammalian cells with green fluorescent protein indicators. *J. Biol. Chem.* **2004**, *279*, 22284–22293, doi:10.1074/jbc.M312847200.

41. Krause, F.S.; Blombach, B.; Eikmanns, B.J. Metabolic engineering of *Corynebacterium glutamicum* for 2-Ketoisovalerate production. *Appl. Environ. Microbiol.* **2010**, *76*, 8053–8061, doi:10.1128/AEM.01710-10.

42. Roenneke, B.; Rosenfeldt, N.; Derya, S.M.; Novak, J.F.; Marin, K.; Krämer, R.; Seibold, G.M. Production of the compatible solute α-d-glucosylglycerol by metabolically engineered *Corynebacterium glutamicum*. *Microb. Cell Fact.* **2018**, *17*, 1–14, doi:10.1186/s12934-018-0939-2.

43. Graf, M.; Zieringer, J.; Haas, T.; Nieß, A.; Blombach, B.; Takors, R. Physiological response of *Corynebacterium glutamicum* to increasingly nutrient-rich growth conditions. *Front. Microbiol.* **2018**, *9*, 1–15, doi:10.3389/fmicb.2018.02058.

44. Xu, G.; Zha, J.; Cheng, H.; Ibrahim, M.H.A.; Yang, F.; Dalton, H.; Cao, R.; Zhu, Y.; Fang, J.; Chi, K.; et al. Engineering *Corynebacterium glutamicum* for the de novo biosynthesis of tailored poly-γ-glutamic acid. *Metab. Eng.* **2019**, *56*, 39–49, doi:10.1016/j.ymben.2019.08.011.

45. Schwarzländer, M.; Dick, T.P.; Meyer, A.J.; Morgan, B. Dissecting redox biology using fluorescent protein sensors. *Antioxidants Redox Signal.* **2016**, *24*, 680–712, doi:10.1089/ars.2015.6266.

46. Van Laer, K.; Buts, L.; Foloppe, N.; Vertommen, D.; Van Belle, K.; Wahni, K.; Roos, G.; Nilsson, L.; Mateos, L.M.; Rawat, M.; et al. Mycoredoxin-1 is one of the missing links in the oxidative stress defence mechanism of *mycobacteria*. *Mol. Microbiol.* **2012**, *86*, 787–804, doi:10.1111/mmi.12030.

47. Liu, Y.B.; Long, M.X.; Yin, Y.J.; Si, M.R.; Zhang, L.; Lu, Z.Q.; Wang, Y.; Shen, X.H. Physiological roles of mycothiol in detoxification and tolerance to multiple poisonous chemicals in *Corynebacterium glutamicum*. *Arch. Microbiol.* **2013**, *195*, 419–429, doi:10.1007/s00203-013-0889-3.

48. El Shafey, H.M.; Ghanem, S.; Merkamm, M.; Guyonvarch, A. *Corynebacterium glutamicum* superoxide dismutase is a manganese-strict non-cambialistic enzyme in vitro. *Microbiol. Res.* **2008**, *163*, 80–86, doi:10.1016/j.micres.2006.05.005.

49. Si, M.; Feng, Y.; Chen, K.; Kang, Y.; Chen, C.; Wang, Y.; Shen, X. Functional comparison of methionine

sulphoxide reductase A and B in *Corynebacterium glutamicum*. *J. Gen. Appl. Microbiol.* **2017**, *63*, 280–286, doi:10.2323/jgam.2017.01.005.

50. Si, M.; Zhang, L.; Chaudhry, M.T.; Ding, W.; Xu, Y.; Chen, C.; Akbar, A.; Shen, X.; Liu, S.J. *Corynebacterium glutamicum* methionine sulfoxide reductase a uses both mycoredoxin and thioredoxin for regeneration and oxidative stress resistance. *Appl. Environ. Microbiol.* **2015**, *81*, 2781–2796, doi:10.1128/AEM.04221-14.

51. Baez, A.; Shiloach, J. *Escherichia coli* avoids high dissolved oxygen stress by activation of SoxRS and manganese-superoxide dismutase. *Microb. Cell Fact.* **2013**, *12*, 1–9, doi:10.1186/1475-2859-12-23.